

# Measuring Amplitude and Frequency Modulations in Noise Using Multiband Energy Operators\*

Alan C. Bovik,<sup>†</sup> Petros Maragos<sup>‡</sup> and Thomas F. Quatieri<sup>§</sup>

<sup>†</sup> *Laboratory for Vision Systems, University of Texas, Austin, TX 78712-1084*

<sup>‡</sup> *Division of Applied Sciences, Harvard University, Cambridge, MA 02138*

<sup>§</sup> *MIT Lincoln Laboratory, 244 Wood Street, Lexington, MA 02173*

**Abstract** - This paper develops the statistical properties of the nonlinear energy operator  $\Psi(s) = (\dot{s})^2 - s\ddot{s}$  and a related energy separation algorithm (ESA). The ESA uses  $\Psi$  to demodulate noisy AM-FM signals. The performance of  $\Psi$  and the ESA when applied to bandpass noisy AM-FM signals is examined. The predicted performance is found to be greatly improved if the local signal frequencies occur within the filter passband. Using this observation, a multiband energy operator and ESA approach is devised. The results suggest that greatly improved practical strategies are feasible for tracking and identifying local pattern coherencies manifested as local concentrations of signal frequencies.

## I. INTRODUCTION

Methods for the accurate and efficient extraction of amplitude modulation (AM) and frequency modulation (FM) information in signals of the form

$$s(t) = a(t) \cos[\phi(t)] \quad (1)$$

are of increased recent interest, owing to heightened use of modulation models for e.g., speech signal production [1], [2] and certain structures in optical images [3]. In (1),  $s(t)$  has time-varying amplitude  $a(t)$  and instantaneous frequency

$$\omega_i(t) = \dot{\phi}(t).$$

where  $\dot{\phi} = d\phi/dt$ . The model (1) is most useful if  $a(t)$ ,  $\omega_i(t)$  do not vary too rapidly [5].

The simple and elegant nonlinear signal operator

$$\Psi(s) = (\dot{s})^2 - s\ddot{s}$$

developed by Teager [1] and systematically introduced by Kaiser [4] is effective for detecting AM and FM modulation information in arbitrary AM-FM signals [5], in speech signals [5], [6] and in its 2-D form, in image signals [7]. Indeed, for AM-FM signals of the form (1),

$$\Psi(s) \approx a^2(t) \omega_i^2(t)$$

$$\Psi(\dot{s}) \approx a^2(t) \omega_i^4(t)$$

with negligible error under general realistic conditions [5], [6]. This motivated the *energy separation algorithm* (ESA):

$$\hat{a}^2(t) = \Psi^2(s) / \Psi(\dot{s}) \quad (2)$$

$$\hat{\omega}_i^2(t) = \Psi(\dot{s}) / \Psi(s) \quad (3)$$

to estimate  $a^2(t)$ ,  $\omega_i^2(t)$ . Maragos, Kaiser, and Quatieri [5], [6] analyzed (2), (3) in detail and developed error bounds, which under general conditions are quite small.

\*ACB was supported by a Texas Instruments grant while on sabbatical at Harvard. PM was supported by NSF Grant MIP-9120624 and a NSF PYI Award. TFQ was supported in part by the Department of the Air Force.

Here we assume the deterministic approximation errors in (2), (3) to be small, and consider the effects of noise on the effectiveness of the operator  $\Psi$  and the ESA. In significant noise,  $\Psi$  is rendered unpredictable and the ESA unreliable. However, multiband prefiltering of the noisy modulated signal can provide greatly improved results.

## II. STATISTICS OF $\Psi$

Next the basic statistical properties of the operator  $\Psi$  applied to a random signal  $n(t)$  are developed. Assume that  $n(t)$  is a zero-mean, stationary Gaussian process with autocorrelation  $R(\tau)$  and spectral density  $\Phi(\omega)$ .

Since  $n(t)$  is Gaussian,  $\dot{n}(t)$  and  $\ddot{n}(t)$  are also, which simplifies the computation of the moments of

$$\Psi(n) = (\dot{n})^2 - n\ddot{n}.$$

Note that

$$\begin{aligned} \text{Var}[n] &= R(0), & \text{Var}[\dot{n}] &= -R^{(2)}(0) \\ \text{Var}[\ddot{n}] &= R^{(4)}(0), & E[n\ddot{n}] &= R^{(2)}(0), \end{aligned}$$

where  $R^{(k)}(\tau) = d^k R(\tau) / d\tau^k$ . Then

$$E[\Psi(n)] = -2R^{(2)}(0) = \frac{1}{\pi} \int_{-\infty}^{\infty} \omega^2 \Phi(\omega) d\omega,$$

the spectral variance of  $n(t)$ . The variance is found for Gaussian  $n(t)$  using Isserlis's formula [8]:

$$\text{Var}[\Psi(n)] = 3 [R^{(2)}(0)]^2 + R(0)R^{(4)}(0).$$

Both increase dramatically with higher frequencies in  $n(t)$ .

Clearly  $\Psi(n)$  can be negative - highly undesirable, in view of the interpretation of  $\Psi$  as energy and the definition of the ESA (2), (3). Positivity of the output of  $\Psi$  has been explored in detail in [9].

Lastly, in evaluating the ESA the statistics of  $\Psi(\dot{n})$  are of use. From the preceding it is easily established that

$$E[\Psi(\dot{n})] = 2R^{(4)}(0)$$

$$\text{Var}[\Psi(\dot{n})] = 3 [R^{(4)}(0)]^2 + R^{(2)}(0)R^{(6)}(0).$$

## III. ENERGY OF BANDPASS AM-FM SIGNALS

Consider the noisy AM-FM signal

$$f(t) = s(t) + n(t)$$

with  $s(t)$  given by (1),  $n(t)$  given in Section II. Define the bandpass filter with center frequency  $\omega_c$ , impulse response

$$g_{\sigma}(t) = 2 h_{\sigma}(t) \sin(\omega_c t), \quad (4)$$

and frequency response

$$G_{\sigma}(\omega) = (1/j) [H_{\sigma}(\omega - \omega_c) - H_{\sigma}(\omega + \omega_c)] \quad (5)$$

where

$$H_\sigma(\omega) = \sigma^{1/2} H(\omega/\sigma),$$

$H(\omega)$  is a low-pass filter with even-symmetric impulse response  $h(t)$  and  $\sigma > 0$  is a bandwidth parameter.

Define the  $k$ th-order spread about  $\omega = \pm\alpha$ :

$$V_H^{(k)}(\alpha) = \frac{1}{2\pi} \left[ \int_{\mathbb{R}} (\alpha \pm \omega)^{2k} |H(\omega)|^2 d\omega \right]^{-2k} \quad (6)$$

minimized at  $\alpha = 0$ :  $V_H^{(1)}(0) = \text{inf} \{ V_H^{(k)}(\alpha) \}$ . Note that

$$V_{H_\sigma}^{(1)}(\alpha) = \sigma V_H^{(1)}(\alpha/\sigma),$$

so the bandwidth of  $H_\sigma(\omega)$  increases linearly with  $\sigma$ .

Assume the  $(+\omega)$ ,  $(-\omega)$  parts of  $G_\sigma(\omega)$  do not overlap:

$$|G_\sigma(\omega)|^2 = |H_\sigma(\omega - \omega_c)|^2 + |H_\sigma(\omega + \omega_c)|^2.$$

We assume constant energy across scales:

$$\frac{1}{2\pi} \int_{\mathbb{R}} |H_\sigma(\omega)|^2 d\omega = 1.$$

Now denote the filtered signal-plus-noise combination

$$f_\sigma(t) = s_\sigma(t) + n_\sigma(t)$$

where  $s_\sigma(t) = s(t) * g_\sigma(t)$ ,  $n_\sigma(t) = n(t) * g_\sigma(t)$ . The rest of this section is devoted to analyzing the bandpass filter / energy operator system depicted in Fig. 1.

### A. Filtered Signal Approximations

The following important approximation is made throughout this paper: if  $s(t) = a(t)\cos[\phi(t)]$  is input to the linear system with frequency response  $G_\sigma(\omega)$  (5), then the response  $s_\sigma(t)$  can be approximated

$$\hat{s}_\sigma(t) = a(t)|G_\sigma[\omega_i(t)]|\cos\{\phi(t) + \angle G_\sigma[\omega_i(t)]\}. \quad (7)$$

For sinusoidal  $s(t)$ , (7) is exact; indeed, (7) is a quasi-extension of the concept of linear system eigenfunction. Generally the error is bounded as follows. First:

$$\Delta_p(g_\sigma) = \left[ \int_{\mathbb{R}} |a(t)|^{2p} |g_\sigma(t)|^2 dt \right]^{1/2}$$

$$\delta(a) = \left[ \int_{\mathbb{R}} |\dot{a}(t)|^2 dt \right]^{1/2}$$

**Theorem 1** - Let  $\varepsilon_s(t) = |s_\sigma(t) - \hat{s}_\sigma(t)|$ . Then

$$\varepsilon_s(t) \leq \frac{4}{3} a_{\max} \Delta_2(g_\sigma) \delta(\omega_i) + 2 \Delta_1(g_\sigma) \delta(a),$$

where  $a_{\max} = \sup |a(t)|$ .  $\blacklozenge$

**Theorem 1** bounds  $\varepsilon_s$  in terms of the duration of  $g_\sigma(t)$  and the smoothness of the AM-FM functions  $a$  and  $\omega_i$  expressed as Sobolev 2-norms [3]. **Theorem 1** also approximates the derivatives of the response  $s_\sigma(t)$ : ( $D^k = d^k/dt^k$ )

$$D^k s_\sigma(t) \approx a(t) |\omega_i(t)|^k |G_\sigma[\omega_i(t)]| \cdot \cos\{\phi(t) + \angle G_\sigma[\omega_i(t)] + k\frac{\pi}{2}\}. \quad (8)$$

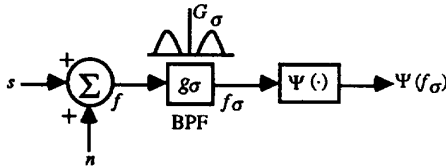


Fig. 1. Block diagram of basic single-band energy operator.

We assume (8) for  $k = 1, 2, 3$ . By **Theorem 1**, the validity of (8) requires that  $\Delta_m(D^k g_\sigma)$ , be small  $k \leq 3$ .

Reasoning similar to **Theorem 1**, approximate the energy  $\Psi$  of the filtered signal component  $s_\sigma(t)$  and its derivative:

$$\hat{\Psi}(s_\sigma) = a^2(t) \omega_i^2(t) |G_\sigma[\omega_i(t)]|^2 \quad (9)$$

and  $\hat{\Psi}(\dot{s}_\sigma) = \omega_i^2(t) \hat{\Psi}(s_\sigma)$ . First define  $\bar{g}_\sigma = \int_{\mathbb{R}} |g_\sigma(t)| dt$ .

**Theorem 2** - Let  $\varepsilon_\Psi(t) = |\Psi(s_\sigma) - \hat{\Psi}(s_\sigma)|$ . Then

$$\varepsilon_\Psi(t) \leq \frac{4}{3} (a_{\max})^2 \delta(\omega_i) \left[ \bar{g}_\sigma \Delta_2(\bar{g}_\sigma) + \bar{g}_\sigma \Delta_2(g_\sigma) + 2 \bar{g}_\sigma \Delta_2(\dot{g}_\sigma) \right]$$

$$+ 2 a_{\max} \delta(a) \left[ \bar{g}_\sigma \Delta_1(\bar{g}_\sigma) + \bar{g}_\sigma \Delta_1(g_\sigma) + 2 \bar{g}_\sigma \Delta_1(\dot{g}_\sigma) \right]. \quad \blacklozenge$$

In **Theorem 2** and the approximations in (8), (10), the errors are small when  $D^k g_\sigma(t)$  is of short duration,  $0 \leq k \leq 3$ .

### B. Filtered Noise Approximations

Denote the autocorrelation of  $n_\sigma(t)$  by  $R_\sigma(\tau)$  with spectrum  $\Phi_\sigma(\omega) = |G_\sigma(\omega)|^2 \Phi(\omega)$ . Of interest are the  $(2k)$ -derivatives of  $R_\sigma(\tau)$  at  $\tau = 0$ :

$$R_\sigma^{(2k)}(0) = \frac{1}{2\pi} \int_{\mathbb{R}} (j\omega)^{2k} |G_\sigma(\omega)|^2 \Phi(\omega) d\omega.$$

An important approximation will often be used:

$$R_\sigma^{(2k)}(0) \approx \hat{R}_\sigma^{(2k)}(\alpha), \quad (11)$$

where for  $\alpha \in \mathbb{R}$

$$\hat{R}_\sigma^{(2k)}(\alpha) = (-1)^k \alpha^{2k} |G_\sigma(\alpha)|^2 \Gamma_\sigma \quad (12)$$

and the filtered noise power:

$$\Gamma_\sigma = \frac{1}{2\pi} \int_{\mathbb{R}} \frac{|G_\sigma(\omega)|^2}{|G_\sigma(\omega_c)|} \Phi(\omega) d\omega.$$

The veracity of (11) is made clear next.

**Theorem 3** - Let  $\varepsilon_n^{(k)}(\alpha) = |R_\sigma^{(2k)}(0) - \hat{R}_\sigma^{(2k)}(\alpha)|$ . Then

$$\varepsilon_n^{(k)}(\alpha) \leq 2\alpha^{2k} \Phi_{\max} \left[ 2\sqrt{2} k \frac{\Phi}{\Gamma_\sigma} V_H^{(1)}\left(\frac{\alpha - \omega_c}{\sigma}\right) \cdot \left\{ \left| \frac{\Phi}{\Gamma_\sigma} \right|^{2k-1} \left[ V_H^{(2k-1)}\left(\frac{\omega_c}{\sigma}\right) \right]^k + 1 \right\} + \left| 1 - \frac{|G_\sigma(\alpha)|^2}{|G_\sigma(\omega_c)|^2} \right| \right]$$

where  $\Phi_{\max} = \sup |\Phi(\omega)|$  and  $V_H^{(k)}$  is given by (6).  $\blacklozenge$

The validity of (11), (12) requires two assumptions. First, the spread  $V_H^{(1)}$  about  $(\alpha - \omega_c)/\sigma$  must be small:  $\alpha$  must fall within the (small) passband of  $G_\sigma$ . Even then  $||G_\sigma(\alpha)| - |G_\sigma(\omega_c)||$  should be small, implying that the in-band amplitude response  $|G_\sigma(\omega)|$  be flat (Fig. 2).

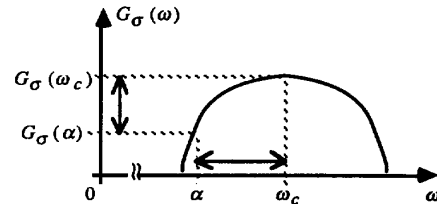


Fig. 2. The validity of (11), (12) requires that the indicated (arrowed) quantities be small.

We use in a specific form of (11). When analyzing  $f_\sigma(t)$  or noise  $n_\sigma(t)$  at time  $t$ , we use (11) with  $\alpha = \omega_i(t)$ :

$$R_\sigma^{(2k)}(0) \approx \hat{R}_\sigma^{(2k)}[\omega_i(t)]. \quad (13)$$

This is a *time-varying* approximation to the autocorrelation of the filtered noise. In using (13), there is a tacit assumption that where  $f_\sigma(t)$  is being analyzed, it is being done so with a filter that is concentrated in the vicinity of  $\omega_i(t)$ .

### C. Filtered Noisy AM-FM Signal Approximations

First note that

$$\Psi(\dot{f}_\sigma) = \Psi(s_\sigma) + \Psi(n_\sigma) + 2\dot{s}_\sigma \dot{n}_\sigma - s_\sigma \ddot{n}_\sigma - \dot{s}_\sigma n_\sigma$$

with zero-mean trailing terms. From (13) the expected energy of the filtered signal-plus-noise is approximately:

$$E[\Psi(f_\sigma)] \approx \omega_i^2(t) |G_\sigma[\omega_i(t)]|^2 [a^2(t) + 2\Gamma_\sigma] \quad (14)$$

$$E[\Psi(\dot{f}_\sigma)] \approx \omega_i^4(t) |G_\sigma[\omega_i(t)]|^2 [a^2(t) + 2\Gamma_\sigma]. \quad (15)$$

Although the ratio of (15) to (14) is an appealing approximation of the expected value of the ESA (2), such an approximation must be carefully justified, particularly since the energy operator may take values near zero.

$$\text{Var}[\Psi(f_\sigma)] \approx 4\omega_i^4(t) |G_\sigma[\omega_i(t)]|^4 \Gamma_\sigma [a^2(t) + \Gamma_\sigma]$$

$$\text{Var}[\Psi(\dot{f}_\sigma)] \approx 4\omega_i^8(t) |G_\sigma[\omega_i(t)]|^4 \Gamma_\sigma [a^2(t) + \Gamma_\sigma].$$

### IV. COMPUTING THE ESA IN NOISE

Here we justify the ESA (2), (3) in the presence of noise, where filtering is applied to reduce the noise contribution. Figure 3 depicts the analyzed ESA system.

#### A. Large SNR ESA Approximations

Define the instantaneous signal-to-noise ratio:

$$\text{SNR}_\sigma(t) = a^2(t) / \Gamma_\sigma.$$

For  $\text{SNR}_\sigma(t)$  large, 2nd-order approximations to the expected ESA (2), (3) are useful:

$$\begin{aligned} E[\hat{\omega}_i^2(t)] &\approx \omega_i^2(t) \left\{ 1 + \frac{4 \text{SNR}_\sigma(t)}{[\text{SNR}_\sigma(t) + 2]^2} \right\} \\ &\approx \omega_i^2(t) \quad (\text{large SNR}), \end{aligned} \quad (16)$$

and

$$\begin{aligned} E[\hat{a}^2(t)] &\approx a^2(t) \left\{ 1 + \frac{10 \text{SNR}_\sigma(t) + 4}{\text{SNR}_\sigma(t) [\text{SNR}_\sigma(t) + 2]} \right\} \\ &\quad \cdot |G_\sigma[\omega_i(t)]|^2 \\ &\approx a^2(t) |G_\sigma[\omega_i(t)]|^2 \quad (\text{large SNR}). \end{aligned} \quad (17)$$

The justifications for (16), (17) and the following are omitted here to conserve space. For the variances of the ESA:

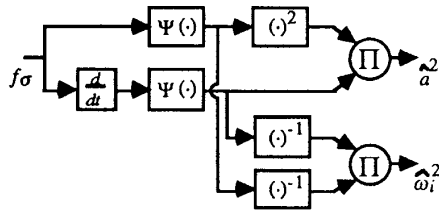


Fig. 3. Diagram of basic ESA with noisy input.

$$\text{Var}[\hat{\omega}_i^2(t)] \approx \omega_i^4(t) \frac{4 [\text{SNR}_\sigma(t) - 1]}{[\text{SNR}_\sigma(t) + 2]^2}, \quad (18)$$

and

$$\text{Var}[\hat{a}^2(t)] \approx 4a^4(t) \frac{5 \text{SNR}_\sigma(t) + 1}{\text{SNR}_\sigma^2(t)} |G_\sigma[\omega_i(t)]|^4. \quad (19)$$

Although the variances (18), (19) increase dramatically with the fourth powers of  $\omega_i(t)$ ,  $a(t)$ , the ratios of (18), (19) to the squares of (16), (17) are negligible at reasonable values of  $\text{SNR}_\sigma(t)$ . Both ratios fall below 0.1 for  $\text{SNR}_\sigma(t) < 34$ . It subsequently follows that for  $\text{SNR}_\sigma(t)$  sufficiently large:

$$\hat{\omega}_i^2(t) \approx \omega_i^2(t) \quad (20)$$

$$\hat{a}^2(t) \approx a^2(t) |G_\sigma[\omega_i(t)]|^2. \quad (21)$$

In (21)  $\omega_i(t)$  may be estimated using (20) then used to compute  $G_\sigma[\omega_i(t)]$ . Another approach is to use filters with flat in-band responses, as discussed earlier.

### V. MULTIBAND FILTERING AND ESA

Figure 4 diagrams a multiband energy operator system. A signal  $f(t)$  passes through multiple filters  $g_m(t)$ ,  $G_m(\omega)$  with  $\omega_m$ ,  $\sigma_m$ , producing outputs  $f_m(t)$ ,  $m = 1, \dots, M$ .

Following filtering, energy demodulation using  $\Psi$  is applied to each output. At each instant  $t$  the response having the maximum *normalized* energy

$$\Psi^*(t) = \max_{1 \leq m \leq M} \frac{\Psi[f_m(t)]}{|G_m(\omega_m)|^2}$$

is input to the ESA. Hence a filter is available with large response, yielding stable computation of the ESA (depicted by dotted lines in Fig. 4).

Criteria for the filters  $g_\sigma$  can be explored in depth; a variety of criteria affect the design. Due to space, these are not fully developed here. Briefly, to reduce the errors in the Theorems, products of the form  $\Delta_1(h)V_H^{(1)}(0)$  be small, suggesting that  $h_\sigma(t)$  be Gaussian. The functions (4) are then Gabor functions. Another important criterion is that the passband of  $H(\omega)$  be approximately flat. This conflicts with a Gabor configuration. While it is interesting to consider the design of low uncertainty filters that have relatively flat passbands, there is no immediately apparent procedure for such a design. In any case, the error bounds in the preceding give worst-case performance.

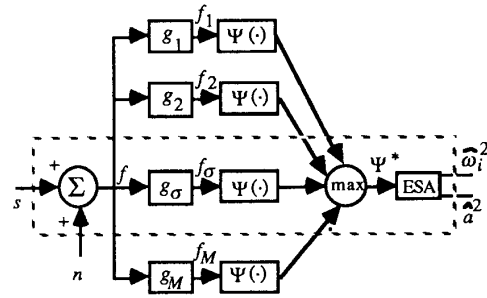


Fig. 4. Multiband filtering and ESA applied to noisy AM-FM signal.

### A. Multiband Filtering

Make the practical assumption that the system of interest produces signals falling in a specific band of frequencies with fixed upper bandlimit  $\Omega_c$ . Others have used time/frequency windows of constant width on a log scale [10], [11]. Theorem 3 gives additional motivation. The modeling error is approximately scaled by  $|\frac{\sigma}{\omega}| 2^{k-1} [V_H^{(2k-1)}(\frac{\omega_c}{\sigma})]^k$ ; to maintain consistent performance across channels, let  $\frac{\sigma_m}{\omega_m} = \text{constant}$ . Also define the subband center frequencies to have 1-octave separation:  $\omega_m = 3 \cdot 2^{-(m+1)} \Omega_c$ ;  $m = 1, \dots, M-1$  and the baseband center frequency:  $\omega_M = 2^M \Omega_c$ .

Assume (sine) Gabor wavelets:

$$G_m(\omega) = \frac{1}{\sqrt{2\pi}\sigma_m} \left[ \exp\left\{-\left(\frac{\omega-\omega_m}{\sigma_m}\right)^2\right\} - \exp\left\{-\left(\frac{\omega+\omega_m}{\sigma_m}\right)^2\right\} \right],$$

which satisfy the usual wavelet admissibility/reconstruction conditions [10], [11]. However, here it is most important that the frequency domain be adequately sampled. One-octave (half-peak BW) filters achieve both prescriptions:

$$\sigma_m = \frac{\omega_m}{3} (\ln 2)^{1/2} = 2^{-(m+1)} (\ln 2)^{1/2} \Omega_c.$$

### VI. EXAMPLE

Assume WLOG that  $\Omega_c = 1$ . Consider a pure chirp signal:

$$s(t) = a_0 \cos(\omega_0 t^2)$$

over the time window  $t \in [1/(2^M \omega_0), 1/(2\omega_0)]$  over which  $\omega_i(t) = 2\omega_0 t$  falls in the band  $[2^{1-M}, 1]$  (avoiding the baseband). First consider the noise-free case. From (9), (10), for the normalized energy of the filter response at time  $t$ :

$$\frac{\Psi(t, m)}{|G_m(\omega_m)|^2} \approx a_0^2 (2\omega_0 t)^2 \cdot \left| \frac{G_m(2\omega_0 t)}{G_m(\omega_m)} \right|^2$$

so, to select the (index of the) analysis channel at time  $t$ :

$$m^*(t) = \arg \max_{1 \leq m \leq M} \left| \frac{G_m(2\omega_0 t)}{G_m(\omega_m)} \right|^2 = \arg \min_{1 \leq m \leq M} |2\omega_0 t - \omega_m|.$$

[assuming  $H(2\omega_0 t + \omega_0) \approx 0$ ]. Then  $m = m^*(t)$  for

$$\left(\frac{9}{16\omega_0}\right) 2^{-m} < t \leq \left(\frac{9}{8\omega_0}\right) 2^{-m}. \quad (22)$$

Now suppose  $s(t)$  is immersed in Gaussian white noise:

$$\Phi(\omega) = \frac{\eta}{\sqrt{2\pi}}; \omega \in \mathbb{R}.$$

Of course, for this noise model, image prefiltering using bandpass filters is an absolute necessity. From Section III-C, for  $m = m^*(t)$ , the normalized energy moments are

$$\frac{E[\Psi(t, m)]}{|G_m(\omega_m)|^2} \approx (2\omega_0 t)^2 (a_0^2 + 4\eta\sigma_m) \cdot \exp\left\{-2\left(\frac{2\omega_0 t - \omega_m}{\sigma_m}\right)^2\right\} \quad (23)$$

$$\frac{\text{Var}[\Psi(t, m)]}{|G_m(\omega_m)|^4} \approx 2\eta\sigma_m (2\omega_0 t)^4 (a_0^2 + 2\eta\sigma_m) \cdot \exp\left\{-4\left(\frac{2\omega_0 t - \omega_m}{\sigma_m}\right)^2\right\}. \quad (24)$$

Expressions for  $\Psi(t, m)$  are the same [multiplied by  $(2\omega_0 t)^2$ ].

Now suppose  $q \neq m^*(t)$ . Determine the normalized out-of-band expected energy using (11) with  $\alpha = \omega_q$ :

$$\frac{E[\Psi(t, q)]}{|G_q(\omega_q)|^2} \approx 2\eta\sigma_q \omega_q^2 \quad (25)$$

### A. Channel Selection

From (22)  $2\omega_0 t > \left(\frac{9}{8}\right) 2^{-m}$  when  $m = m^*(t)$ , so the ratio of (23) to (25) is bounded below by  $\left(\frac{9}{16}\right) 2^{3q-2m} \sqrt{\ln 2} \text{snr}_0$ ,

where  $\text{snr}_0 = \left(\frac{a_0^2}{\eta}\right)$ . For  $\text{snr}_0$  large, the in-band channel will dominate the noise channels. However, it should be observed that  $\Psi$  can be sensitive when a low frequency signal is to be detected in high-frequency noise.

### B. ESA Computation

If the correct channel is selected, the ratio of the square of (23) to (24) to the is bounded below by  $2^m \sqrt{\ln 2} \text{snr}_0$ . So, for reasonably high  $\text{snr}_0$  the normalized energies satisfy

$$\frac{E[\Psi(t, m)]}{|G_m(\omega_m)|^2} \approx a_0^2 (2\omega_0 t)^2$$

$$\frac{E[\Psi(t, m)]}{|G_m(\omega_m)|^2} \approx a_0^2 (2\omega_0 t)^4.$$

As desired the ESA will then yield for  $t$  satisfying the above:

$$\hat{\omega}_i^2(t) \approx (2\omega_0 t)^2 \quad \hat{a}^2(t) \approx a_0^2$$

### VII. FUTURE WORK

Future work includes digital versions using the discrete-time energy operator [4] and extensions to allow the analysis of multi-component AM-FM signals:

$$s(t) = \sum_{k=1}^K a_k(t) \cos[\phi_k(t)]. \quad (26)$$

This will involve tracking multiple components that merge, vanish, or contain discontinuities. Although the problem is difficult, the model (26) may find widespread application.

### REFERENCES

- [1] H.Teager & S.Teager, "Evidence for nonlinear speech production mechanisms in the vocal tract," *NATO Adv. Study Inst. Speech Prod. Speech Model.*, France, 1989.
- [2] P.Maragos, T.Quatieri & J.Kaiser, "Speech nonlinearities, modulations, and energy operators," *Proc. ICASSP*, Toronto, 1991.
- [3] A.Bovik, N.Gopal, T.Emmott & A.Restrepo, "Localized measurement of emergent image frequencies by Gabor wavelets," *IEEE Trans. IT-38*, 691-712, 1992.
- [4] J.Kaiser, "On a simple algorithm to calculate the 'energy' of a signal," *Proc. ICASSP*, 1990.
- [5] P.Maragos, T.Quatieri & J.Kaiser, "On separating amplitude from frequency modulations using energy operators," *Proc. ICASSP*, San Francisco, 1992.
- [6] P.Maragos, T.Quatieri & J.Kaiser, "Energy separation in signal modulations with application to speech analysis," *Tech. Rept.*, Harvard Robotics Lab., 1991.
- [7] P.Maragos, A.Bovik & T.Quatieri, "A multidimensional energy operator for image processing," *Proc. SPIE Symp. Visual Commun. Image Process.*, Boston, 1992.
- [8] L.Isserlis, "On a formula for the product-moment coefficient of any order of a normal frequency distribution in any number of variables," *Biometrika*, vol. 12, 134-139, 1918.
- [9] A.Bovik & P.Maragos, "Conditions for positivity of an energy operator," *IEEE Trans. SP*, submitted.
- [10] I.Daubechies, "The wavelet transform, time frequency localization and signal analysis," *IEEE Trans. IT-36*, 961-1005, Sept. 1990.
- [11] S.Mallat, "Multifrequency channel decompositions of images and wavelet models," *IEEE Trans. ASSP-37*, 2091-2110, Dec. 1989.